Journal homepage: http://gwse.iheg.org.cn

Research Article

Removal of 1,2,3-Trichloropropane from groundwater using Graphene Oxide-Modified Nano Zero-Valent Iron Activated Persulfate

Hui Li[1,2], Lu Liu[3], Jia-hui Li[2,4], Bai-zhong Yan[5,6], Xiang-ke Kong[1,2*], Wei Zhang[1,2]

[1] *Institute of Hydrogeology and Environmental Geology*, *Chinese Academy of Geological Sciences*, *Shijiazhuang* 050061, *China*.
[2] *Key Laboratory of Groundwater Contamination and Remediation*, *China Geological Survey (CGS)* & *Hebei Province*, *Shijiazhuang* 050061, *China*.
[3] *Institute of Geological Environment Monitoring Hebei Province*, *Shijiazhuang* 050031, *China*.
[4] *Chinese Academy of Geological Sciences*, *Beijing* 100037, *China*.
[5] *School of Water Resources and Environment*, *Hebei Geology University*, *Shijiazhuang* 050031, *China*.
[6] *Hebei Province Collaborative Innovation Center for Sustainable Utilization of Water Resources and Optimization of Industrial Structure*, *Shijiazhuang* 050031, *China*.

Abstract: Graphene Oxide (GO), nanoscale Zero-Valent Iron (nZVI) and GO-modified nZVI (GO-nZVI) composite materials were prepared by the Hummer and polyphenol reduction method, respectively, and Scanning Electron Microscope (SEM) and X-ray Diffraction (XRD) were used to characterize the morphology and phase composition of these materials. A series of batch experiments were then conducted to investigate the performance and influencing factors of GO-nZVI activating peroxydisulfate (SPS) for the degradation of 1,2,3-trichloropropane (TCP). Finally, an in-situ oxidation reaction zone was created by GO-nZVI-activated SPS in a one-dimensional simulated system to study the remediation of TCP contamination under different aquifer conditions. The results showed that the GO-nZVI composite exhibited a porous, fluffy structure, with spherical nZVI particles loaded onto the surface and folds of the GO sheets. Compared with unmodified nZVI particles, the GO-nZVI composite significantly enhanced the removal efficiency of TCP by activated SPS, achieving a removal rate of 67.2% within an hour - 78.2% higher than that of the unmodified system. The SPS dosage and the C/Fe ratio in GO-nZVI were found to significantly affect the degradation efficiency of TCP. The removal rate of TCP increased with higher SPS concentration, and a 10% carbon addition, yielded the best activation effect. The one-dimensional simulation results indicated that the removal rate of TCP ranged from 30.1% to 73.3% under different conditions. A larger medium particle size and higher concentrations of reactants (SPS and GO-nZVI) improved pollutant degradation efficiency, increasing TCP removal by 62.1%, 23.8%, and 3.7%, respectively. In contrast, a higher groundwater flow velocity was not conducive to the removal of pollutants, with the TCP removal rate decreasing by approximately 41.9%.

Keywords: Graphene oxide; Nanoscale zero-valent iron; Persulfate; 1, 2, 3-Trichloropropane; Groundwater; In-situ reaction zone

Received: 13 Feb 2025/ Accepted: 21 Aug 2025/ Published: 10 Oct 2025

Introduction

Chlorinated organic compounds are difficult to degrade and some of them have carcinogenic, teratogenic, mutagenic, and other toxic effects. Chlorinated hydrocarbons rank first on China's black list of 68 priority pollutants (Ren et al. 2021). As a synthetic chlorinated hydrocarbon pollutant, 1,2,3-trichloropropane (TCP) is a major

*Corresponding author: Xiang-ke Kong, *E-mail address*: kongxiangke@mail.cgs.gov.cn

DOI: 10.26599/JGSE.2025.9280058

Li H, Liu L, Li J H, et al. 2025. Removal of 1,2,3-Trichloropropane from groundwater using Graphene Oxide-Modified Nano Zero-Valent Iron Activated Persulfate. Journal of Groundwater Science and Engineering, 13(4): 341-351.

by-product of epichlorohydrin production during industrial processes (Merrill et al. 2019; Boyandin et al. 2024), and its output continues to grow with the increasing demand for epichlorohydrin each year. The problem of groundwater pollution caused by "running, emitting, dripping, and leaking" during the synthesis, transportation, and storage of TCP has attracted increasing concern. Characterized by moderate solubility and strong stability, TCP can rapidly migrate from soil to groundwater once released, resulting in persistent groundwater pollution (Dai et al. 2023; Zhang et al. 2023) and posing a serious threat to the ecological environment and human health. Therefore, TCP pollution is an important focus in research on chlorinated hydrocarbons organic pollutants.

At present, many studies have been conducted on remediation techniques for water contaminated with chlorinated hydrocarbons both domestically and internationally, and the majority of studies on TCP remediation have focused on biodegradation technology (Li et al. 2023; Ning et al. 2022). However, this approach still faces problems such as a limited number of effective bacterial strains, a low reaction rate, and a long remediation cycle (Shang et al. 2022). Zero-Valent Iron (ZVI) is not only capable of reducing various chlorinated organic compounds in the environment but is also readily available and inexpensive, making it increasingly widely used in the field of environmental remediation (Xue et al. 2023; Plessl et al. 2023; Li et al. 2023). Nonetheless, many studies have revealed that ZVI with different particle sizes has a low TCP degradation efficiency and may hardly experience reduction reactions. This is mainly because the Cl-Cl bond in TCP has a high dissociation energy, making it difficult for ZVI to provide the activation energy required for dechlorination (Sarathy et al. 2010; Li et al. 2015).

Advanced oxidation technologies, especially those using ferrous iron to activate persulfate, are attracting increasing attention due to their advantages of a short remediation cycle, rapid effect, and low cost (Jiang et al. 2024; Arslan-Alaton and Koba-Ucun, 2023; Wang et al. 2022; Li et al. 2015). A growing number of researchers have recently attempted to apply nZVI materials in advanced oxidation processes to replace Fe(II) as an activator, which can address the problems of rapid oxidation of Fe(II) to Fe(III) and the low activation efficiency of persulfate (Yu et al. 2023).

The method of using nZVI activated persulfate can achieve fairly satisfactory results in remediating water polluted by unsaturated chlorinated hydrocarbons (such as trichloroethylene). However, for TCP pollution and other saturated chlorinated alkane, it can only improve pollutant removal efficiency to a certain extent due to limited reaction and mass transfer rates and a single degradation pathway, and it requires a large dosage of oxidant during reaction (Li et al. 2015).

In terms of preparing nZVI as an activator, the use of plant polyphenol extract as Fe^{3+} reductant can significantly reduce the cost, and the polyphenols are environmentally friendly posing no risk of secondary pollution. In addition, when added to the persulfate oxidation system, the polyphenol can also serve as an activator to generate sulfate radicals by directly activating peroxydisulfate ($S_2O_8^{2-}$) (Li et al. 2015; Zhang, 2019). It has been reported that polyphenol-coated nZVI itself has a low reduction efficiency for chlorinated hydrocarbons, mainly due to lower electron transport efficiency.

Ongoing research on graphene-based materials has uncovered that these materials possess excellent adsorption and electron transport capabilities. Graphene and its derivatives have demonstrated outstanding performance in removing heavy metals and organic pesticides when loaded with nZVI (Yang et al. 2018; Ren, 2019; Braki et al. 2024; Liu et al. 2022). However, the effectiveness of these materials for degrading chlorinated organic compound pollution has rarely been verified (Huang et al. 2023).

In summary, the existing redox technologies for treating TCP and other chlorinated hydrocarbons that are difficult to degrade in water, including nZVI/modified nZVI and activated persulfate, still face challenges such as the need for large dosage of reactants, a single degradation pathway, low reaction and mass transfer rates, and an unsatisfactory remediation effect. Regarding this issue, this study aims to take advantage of advanced oxidative remediation techniques using nZVI injection and persulfate, and to utilize Graphene Oxide (GO) as a carrier for nZVI, thereby preparing a GO-modified nZVI (GO-nZVI) composite. The efficiency of the composite in catalyzing persulfate to remove TCP from water and the effects of persulfate and GO dosage were investigated. Furthermore, an in-situ reaction zone using GO-nZVI to activate persulfate was simulated and created to explore its remediation effect on TCP in groundwater. The influence of medium particle size, groundwater flow velocity, and the injection concentrations of SPS and GO-nZVI on TCP removal efficiency were also analyzed, providing a theoretical basis for applying advanced oxidation technology to the treatment of chlorinated hydrocarbon pollution in groundwater.

1 Materials and methods

1.1 Experimental materials

Graphite powder (80–120 mesh, 99.9% purity) and 0.22 μm filtration membranes were purchased from Shanghai Macklin Biochemical Technology Co., Ltd. Ordinary green tea leaves were sourced from Chunxiang Tea Farm (Shihe District, Xinyang City, Henan Province, China). TCP, sulfuric acid, potassium permanganate, sodium nitrate, Sodium PerSulfate (SPS), ferric chloride, ferrous sulfate, calcium chloride, hydrochloric acid, hydrogen peroxide, sodium hydroxide, methanol, and ethanol of analytical grade were supplied by chemical reagent companies in Beijing. Quartz sand, purchased from Henan Zhengyuan Chemical Co., Ltd, was screened using a 10–200 mesh standard sieve, washed with deionized water to remove surface dust, sterilized at high temperature using a high-pressure sterilizer, and then dried for later use. Test water was prepared according to the concentration of common ions found in groundwater, as listed in Table 1.

1.2 Preparation and characterization of GO, nZVI and GO-nZVI

A suitable amount of 98% concentrated sulfuric acid was added into a 250 mL beaker, then graphite powder and sodium nitrate were added at a mass ratio of 2:1, followed by mechanical stirring in an ice water bath for 20 minutes. After that, an appropriate amount of potassium permanganate, generally 2-3 times the mass of the graphite powder, was slowly added to the mixture. The mixture was then transferred to a thermostatic water bath at 35°C and maintained for 40 minutes. After adding 100-200 mL of ultrapure water, the mixture was transferred to a 98°C thermostatic water bath for 15 minutes. Subsequently, the mixture was diluted with warm water, combined with 25 mL of 30% hydrogen peroxide, then filtrated and washed three times, followed by vacuum drying at 70°C for 12 hours. Finally, the brown material GO was obtained for later use.

2 g of green tea were added to 50 mL of water, heated at 80°C for 30 minutes, and then allowed to stand until reaching room temperature. The tea leaves and extract were then separated using a suction filter. Next, 0.5 g of synthesized GO was fully dispersed in the polyphenol extract by ultrasound for 2 hours to obtain a suspension. Afterward, 50 mL of 0.1 mol/L ferric chloride solution was prepared and slowly added to the GO-polyphenol suspension under constant stirring, followed by reaction for 4 hours. The product was washed with absolute ethanol more than three times and then dried at 60°C under vacuum to obtain GO-nZVI. At the same time, green tea-reduced nZVI (withtout the addition of GO) was prepared in a separate polyphenol extract solution for comparative analysis in subsequent experiments.

To clarify the surface properties of different nanomaterials, a scanning electron microscope (SEM, SU8000, Hitachi, Japan) operating at an accelerating voltage of 3.0 KV was employed to observe the microstructure, surface structure, and dispersion of GO, nZVI, and GO-nZVI. An appropriate amount of each sample was placed on black adhesive tape and subjected to metal spraying. The crystal structures of the materials were analyzed using an X-ray Diffractometer (XRD, Rigaku SmartLab SE, Japan). GO was continuously scanned with characteristic Cu-Kα X-ray diffraction, while nZVI and GO-nZVI were continuously scanned with characteristic Co-Kα X-ray diffraction. The diffraction angle, scanning step size, and working current were set to 10°–90° (2θ), 0.02°, and 40 mA, respectively.

1.3 Batch degradation experiments

Experiments were implemented in a series of 100-mL conical flasks. Specifically, a proper amount of the prepared GO-nZVI (with a GO mass ratio of 10% in the composite) was fully dispersed in deionized water by ultrasonication, after which a 2 g/L TCP stock solution was added to reach a final concentration of 100 mg/L. After mixing, SPS was added to achieve a molar concentration ratio of $S_2O_8^{2-}$, Fe and TCP of 20:5:1. The mixture was oscillated in a thermostatic oscillator (25°C) at 150 rpm. Samples were taken at regular intervals, and free radicals were quenched with absolute methanol. The samples were then filtrated using 0.22 μm filtration membranes. Subsequently, the

Table 1 Parameters of test water（mg/L）

pH	Na^+	Ca^{2+}	Mg^{2+}	SO_4^{2-}	Cl^-	HCO_3^-	NO_3^-	Fe
6.5	30.50	50.20	42.17	120.45	105.30	88.27	1.53	0.04

residual TCP concentration was determined by Gas Chromatograph (GC). A control group was established to investigate the effects of different reaction agents (GO, nZVI, SPS, GO-nZVI, and nZVI + SPS) on TCP removal efficiency. In the above experiments, one group of blank samples and two groups of parallel samples were set up.

The dosage of chemical agents directly affects the reaction efficiency. In this study, the dosage of persulfate was adjusted to obtain molar concentration ratios of $S_2O_8^{2-}$, Fe, and TCP of 30:5:1, 20:5:1, and 10:5:1, respectively, to explore the impact of oxidant dosage on TCP removal efficiency. During the preparation of GO-nZVI, composites with varying Carbon (C)/Fe ratios were obtained by adding different amounts of GO, thereby investigating the TCP removal efficiency of GO-nZVI-activated SPS when the GO dosage was 5%, 10%, and 15%.

1.4 Simulated column experiments

The simulation experiment was carried out using one-dimensional organic glass columns (Fig. 1), each measuring 40 cm in length and 8 cm in diameter, with water distribution plates installed at both ends to ensure the uniform distribution of groundwater in the aquifer medium. The columns were placed horizontally, and Sampling Ports 1, 2, 3 and 4 were set up at equal intervals along the column. Among them, Sampling Port 2 was connected with an injector and served both as the inlet for GO-nZVI suspension and SPS solution, and as the sampling port at the end of injection. Sampling Ports 1 and 4 were used as the upstream and downstream monitoring points. Sampling Port 3 served only as a backup sampling port, to be used when necessary (e.g. in case of blockage of an adjacent sampling port), as it was located close to Sampling Port 2. The outlet of the simulated columns was the final sampling port, which was connected to a three-way tube via a hose. Sampling was completed by adjusting the height of the hose to control the groundwater outlet level.

The medium was packed into the simulated columns, tamped layer by layer, and saturated with 100 mg/L TCP solution. When the concentration of TCP in the effluent was consistent with that in the influent, GO-nZVI suspension and SPS solution (50 mL each) were injected into the saturated medium using all-glass injectors through the injection port (Sampling Port 2), with the injector needles placed at the lower, middle and upper parts of the simulated columns to ensure the agents were distributed as uniformly as possible throughout the medium. After the remediation agents were injected, the flow rate was kept constant, and samples were collected at regular intervals to determine TCP concentration.

A series of simulated columns were prepared, and the medium particle size, groundwater flow velocity, SPS concentration, and GO-nZVI injection concentration were adjusted to explore the effects of these factors on the performance of reaction zone. The experimental parameters of the simulated columns are presented in Table 2.

1.5 TCP testing method

A GC (Shimadzu Plus 2010, Japan) equipped with a Flame Ionization Detector (FID) and automatic headspace sampler (Agilent Technologies G1888)

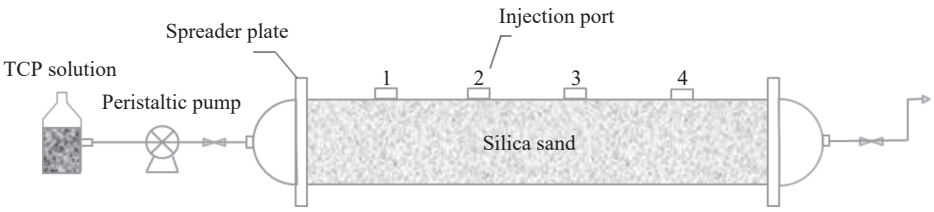

Fig. 1 Schematic diagram of remediation for TCP-contaminated groundwater with in-situ reaction zone

Table 2 Parameters of simulated column tests

Columns	Medium size /mm	Velocity of groundwater flow /m/d	Concentration of SPS /g/L	Concentration of GO-NZVI /g/L
1	0.5–1	0.12	35	10
2	0.1–0.25	0.12	35	10
3	0.5–1	0.25	35	10
4	0.5–1	0.12	50	10
5	0.5–1	0.12	35	20

was employed to measure the TCP content under the following conditions: An HP-PLOT/Q capillary column; column temperature held at 50°C for 2 minutes and then increased at 40°C/min to 220°C for 6 minutes; inlet temperature of 150°C; no split injection; direct injection mode; FID temperature of 350°C; carrier gas (nitrogen) flow rate of 1.5 mL/min; automatic sampler heated to 80°C for 10 minutes; ambient temperature of 23°C; and relative humidity of 20%.

2 Results and discussion

2.1 Characterization of GO, nZVI and GO-nZVI

Characterization analysis was conducted on the different remediation materials. As shown in Fig. 2, the nZVI particles produced via polyphenol reduction were spherical, with an average particle size of 20–30 nm and good dispersity. They did not agglomerate into large particles or form chains connected by magnetic interactions between particles (Fig. 2a). GO displayed as a typical laminated structure (Chen et al. 2020; Horlu et al. 2024) with contorted folds and no surface attachments (Fig. 2b). After loading nZVI, the surface of GO became rougher, and the spherical nZVI particles were distributed on the flat surface of GO or embedded within its folds (Fig. 2c). Some nZVI particles still agglomerated into chains or large granular crystals. These observations suggest that during the loading process, GO disrupts the dispersion stability of the original nZVI particles to some extent, allowing nZVI to enter the interlayers of GO, resulting in a porous, fluffy composite structure.

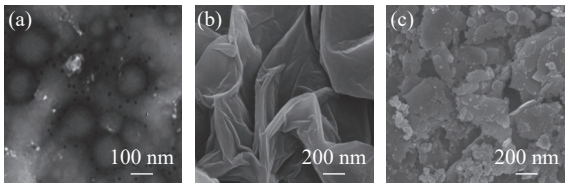

Fig. 2 SEM images of nZVI (a), GO (b) and GO-NZVI (c)

The crystal structures of GO, nZVI and GO-nZVI were analyzed and compared by XRD. The results (Fig. 3) indicate that GO showed a single diffraction peak, with the strongest characteristic peak (002) appearing at 2θ=11.2°, corresponding to the orderly laminated structure of GO. In addition, the interlayer spacing calculated using the Bragg equation was 0.790 nm, which is larger than that of ordinary graphite powder (0.337 nm). This is because the presence of oxygen-containing functional groups on the surface increases the interlayer spacing of GO, implying that GO can provide more space for loading metal nanoparticles.

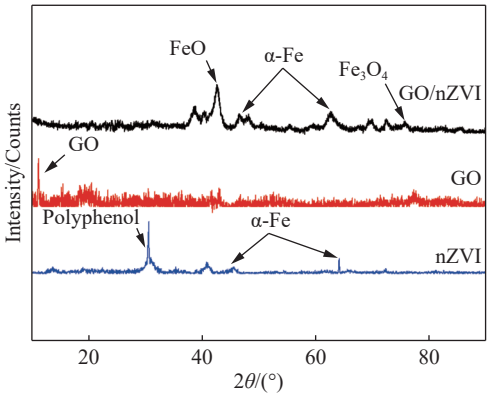

Fig. 3 XRD patterns of nZVI, GO and GO-NZVI

The crystals of nZVI and the GO-nZVI composite exhibited characteristic diffraction peaks of α-FeO at 44.77° (110) and 65.10° (200), respectively, whereas the characteristic peak of GO nearly disappeared, suggesting that GO is completely exfoliated during the preparation of the composite. nZVI also showed a distinct characteristic peak at 32.39°, which might belong to a polyphenol organic compound encapsulated on the surface of nZVI (Deng et al. 2019). In addition, a small amount of Ferrous Oxide (FeO), Hydroxyl-Ferric Oxide (FeOOH) and Ferroso-ferric Oxide (Fe_3O_4) observed in the spectra may have formed due to Fe oxidation during the preparation of nZVI and GO-nZVI.

2.2 TCP removal efficiency by GO-nZVI activated persulfate

To investigate the TCP removal efficiency by GO-nZVI activated persulfate, a comparison was made of the effects of GO, nZVI, GO-nZVI, SPS, and GO-nZVI + SPS on TCP removal in this experiment, with an initial solution pH of 6.5 and an initial TCP concentration of 100 mg/L. As shown in Fig. 4, nZVI alone had almost no effect on TCP removal within 120 minutes. This is because nZVI typically achieves the reductive degradation of organic pollutants only under acidic conditions (Dombek et al. 2004). Compared to common chlorinated hydrocarbons, TCP is more difficult to dechlorinate, requiring chemical remediation agents with higher surface reactivity. Sarathy et al. (2010) found that reactive nZVI with diverse morphologies can achieve some degradation of TCP, but its efficiency remains much lower than

the effective remediation efficiency needed for in-situ applications.

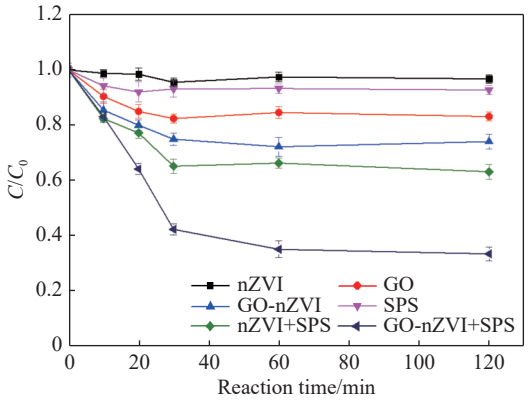

Fig. 4 Removal effect of TCP in different reaction systems

GO alone exhibited a certain surface adsorption effect on TCP, resulting in a TCP removal rate of about 17.8%. After loading nZVI onto GO, the adsorption capacity of GO-nZVI for TCP was significantly higher than that of GO or nZVI alone. The possible reason is that, on the one hand, nZVI particles entering the layered structure of GO enhances its pore structure and increases its specific surface area, thereby strengthening its pollutant adsorption capacity (Xing, 2020). On the other hand, the adsorption capacity and electron transfer capability of GO facilitate the reduction of TCP by nZVI. In other words, GO-nZVI excerts a synergistic effect that enhances both adsorption and reduction of TCP.

Single SPS exhibited only a weak oxidizing effect on TCP. Existing studies have demonstrated that persulfate produces $S_2O_8^{2-}$ with oxidative properties in water through ionization. However, persulfate generally has an insignificant oxidation effects on organic compounds at room temperature due to the low reaction rate (Yan et al. 2008; Xue et al. 2024). The persulfate activated by GO-nZVI evidently improved TCP degradation efficiency, increasing the removal rate from 8.5% to 67.2%. The removal of TCP by GO-nZVI activated SPS was a highly efficient and rapid reaction process, reaching equilibrium and stability within 1–2 hours.

2.3 Influence of persulfate dosage on TCP removal efficiency

When the molar ratio of $S_2O_8^{2-}$ to TCP increased from 10:1 to 30:1, the degradation efficiency of TCP improved from 48.6% to 71.2% (Fig. 5), indicating that the dosage of SPS had a relatively obvious positive correlation with pollutant degradation efficiency. However, different dosage resulted in varying degrees of improvement in TCP degradation. For example, the TCP removal efficiency increased by 36.8% when the molar ratio of $S_2O_8^{2-}$ to TCP increased from 10:1 to 20:1, while it increased by merely 7.1% when the ratio rose from 20:1 to 30:1. This is probably because the activation efficiency of the fixed amount of GO-nZVI on persulfate nearly reaches its maximum at a molar ratio of 5:20, so further increasing the persulfate dosage has little effect on enhancing TCP oxidation efficiency.

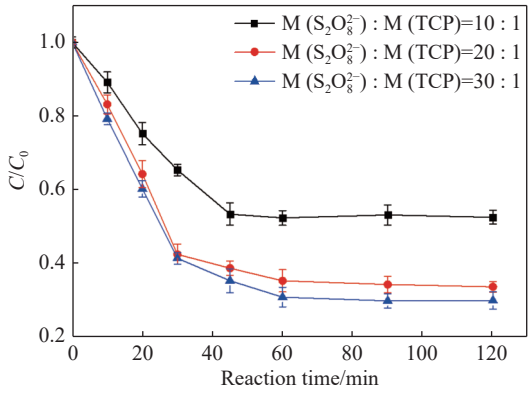

Fig. 5 Removal effect of TCP at different oxidant dosages

Moreover, although increasing the oxidant dosage can improve pollutant removal efficiency to a certain extent, excessive oxidant may damage the physicochemical and biological properties of groundwater, increase sulfate levels, and cause acidification, which in turn affects the subsequent microbial activity and pollutant degradation. Therefore, in practical application, the appropriate dosage of oxidizing agents should be determined by fully considering economic cost, remediation effectiveness, and potential impacts on the groundwater environment.

2.4 Influence of C/Fe ratio in GO-nZVI on TCP removal efficiency

To explore the impact of different C/Fe ratios in GO-nZVI on TCP removal efficiency, GO-nZVI composites with three different GO locadings, namely GO-nZVI^1 (with 5% GO added), GO-nZVI^2 (with 10% GO added), and GO-nZVI^3 (with 15% GO added), were applied to activate SPS to degrade TCP. As shown in Fig. 6, GO-nZVI^3 had the weakest activation effect on SPS, followed by GO-nZVI^1 and then GO-nZVI^2. The nZVI content in GO-nZVI determines the activation degree of

SPS. Specifically, increasing the proportion of nZVI can promote the generation of free radicals and thus accelerate the oxidative degradation of TCP.

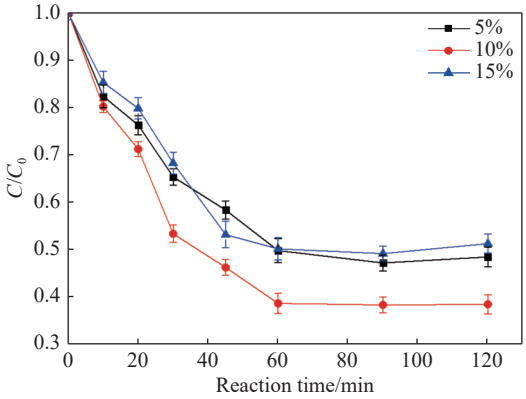

Fig. 6 Removal effect of TCP at different C dosage

Furthermore, the dispersion or immersion of nZVI particles into the layered structure of GO can increase the specific surface area and pore size of the composite, enhancing its synergistic adsorption/oxidation effect on TCP. Therefore, the TCP removal efficiency may increase with higher nZVI loading up to a certain point. However, when the nZVI content was further increased, the TCP removal rate declined slightly. This may be due to the depletion of sulfate radicals by excessive nZVI (Liu, 2018), resulting in reduced oxidative degradation efficiency. Additionally, excessive nZVI can occupy the pore structure of GO and hinders mass transfer process with pollutants (Sun et al. 2023).

2.5 Effectiveness of the reaction zone of GO-nZVI activated persulfate in removing TCP from groundwater

The effectiveness of the reaction zone formed by GO-nZVI activated persulfate in removing TCP from groundwater was investigated in simulated columns, and the results are shown in Fig. 7. TCP concentration at Port 1 did not change significantly since Port 1 was located upstream of the injection port and thus the pollutant concentration was less affected by the injected agents. The concentration of TCP in groundwater dropped markedly in downstream sampling ports within 96 hours, with Port 2 showing the most obvious decrease, followed by Port 3 and then the outlet.

The pollutant degradation efficiency at different sampling ports decreased as the distance from the injection port increased, with average TCP concentration reductions of 56.0%–73.3%, 42.3%–68.6% and 30.1%–64%, respectively. After the reaction zone had operated for a few days, its oxidizing capacity began to decline, and the TCP concentration in the column gradually increased, eventually

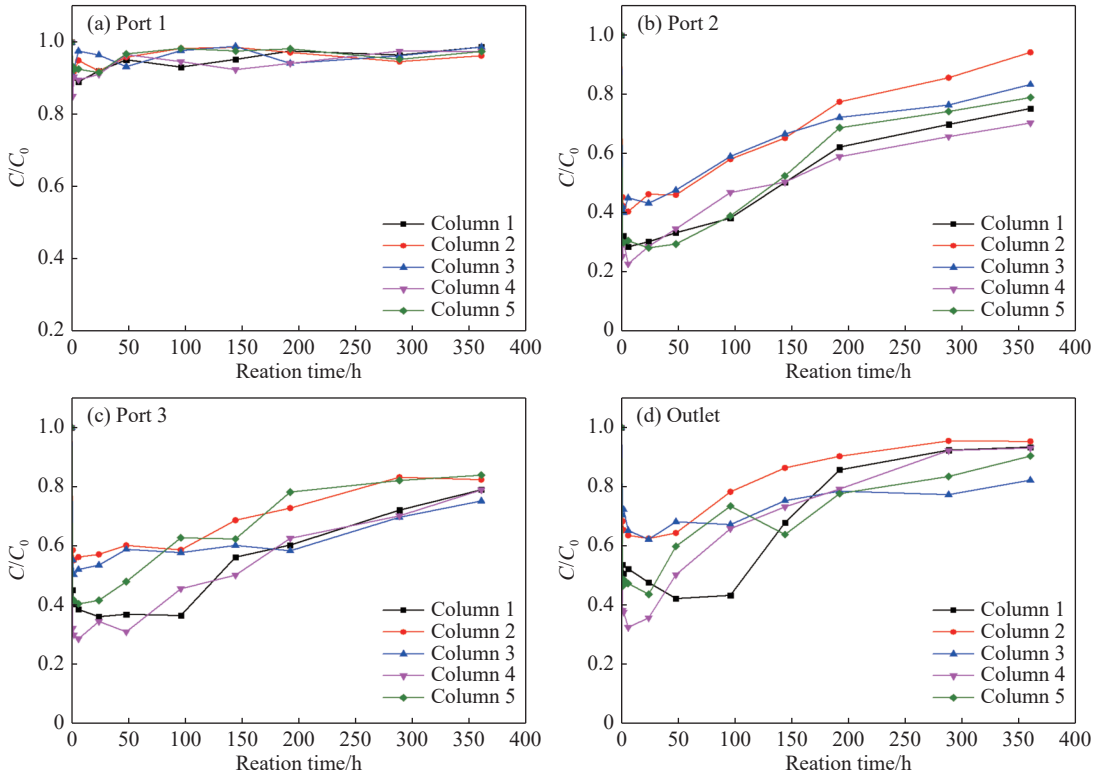

Fig. 7 Changes in TCP concentration at each sampling port in the simulated columns

approaching that of the feed water. This indicates that the remediation capacity of the reaction zone diminishes over time, and the reaction zone ultimately loses its effectiveness once the TCP concentration in the effluent becomes roughly equal to that in the feed water.

The influencing factors for the reaction were analyzed in detail using the changes in TCP concentration at the outlet of each column in Fig. 7(d) as an example. According to the TCP concentration variation curves of columns 1 and 2, the TCP removal efficiency in coarse sand was remarkably higher than that in fine sand. This is because coarse sand has a larger pore space, which allow GO-nZVI to exhibit better mobility, enabling it to form a larger reaction zone along the groundwater flow direction (Li et al. 2015). This improves persulfate activation and enhances oxidation efficiency, resulting in a more effective TCP degradation.

This figure also shows that the TCP concentration began to rise and the remediation efficiency of the reaction zone started to decline after 144 hours of operation in coarse sand. In contrast, the TCP concentration in fine sand started to rebound after only 96 hours, implying that coarse sand provides better sustainable remediation performance. This is likely related to the variations in the permeability of the media. Fine sand has relatively low permeability, and the oxidation products of nZVI further reduce the permeability of the GO-nZVI reaction zone, thus hindering its electron and mass transfer performance and reducing its oxidation efficiency.

It was evident from the TCP concentration variation curves in the effluent of columns 1 and 3 that the average TCP removal rates were 51.8% and 30.1% at groundwater flow velocities of 0.12 m/d and 0.25 m/d, respectively. This suggests that the TCP removal efficiency by oxidation is unsatisfactory at higher groundwater flow velocities. This is because a higher flow velocity does not allow pollutants and persulfate to remain in the GO-nZVI reaction zone long enough for complete reactions, resulting in reduced persulfate activation and lower oxidation efficiency. Although the figure shows that Column 3 had a lower TCP removal efficiency, the TCP removal rate in the effluent only began to decline after 144 hours of operation, and the rate of TCP concentration rebound was slower than that in column 1. This indicates that a higher groundwater flow velocity can, to some extent, improve the sustainable remediation performance of the reaction zone.

By comparing the TCP concentration variation curves in the effluent of Column 1, 4 and 5, it was discovered that the average TCP removal rates in these columns were 51.7%, 64.0% and 53.6%, respectively, representing increases of 23.8% and 3.7% in Columns 4 and 5 compared with Column 1. This suggests that the TCP removal efficiency in the reaction zone increases with higher concentrations of the agents (SPS and GO-nZVI). In addition, the removal rate of TCP was more strongly affected by the concentration of SPS than by that of GO-nZVI. However, after 24 hours, the TCP concentration in Columns 4 and 5 began to rebound, indicating that a high concentration of agents can reduce the sustainable remediation performance of the reaction zone. This may be because greater amounts of oxidation products generated under lager agents concentrations reduce the activation efficiency of SPS, ultimately leading to a decline in the remediation capacity of the reaction zone.

Subsequently, the molar ratio of persulfate actually participating in the reaction was calculated based on the TCP concentration variation curves in the effluent of each column. The time intervals with stable oxidation efficiency in the reaction zone were determined as the reaction time periods for calculation in each column. Specifically, the reaction time periods used were 0–96 h, 0–48 h, 0–192 h, 0–24 h, and 0–24 h for Columns 1–5, respectively. In addition, the average TCP removal efficiency within these periods was determined for each column. The molar ratios of persulfate actually reacting with TCP in the five columns were 8.65:1, 25.70:1, 5.74:1, 38.9:1 and 27.2:1, respectively.

These results illustrate that in the remediation of TCP pollution in groundwater using an in-situ reaction zone of GO-nZVI activated persulfate, the actual utilization rate of the SPS is relatively low, and it is difficult to achieve satisfactory remediation results simply by increasing the dosages of oxidizing agents and activators. To address this issue, current research primarily focuses on improving the performance of oxidants and activators while reducing environmental risks through the following approaches:

(1) Improving the oxidant activation method. This is a major research focus and also an objective of this study. By leveraging the pollutant enrichment and electron transport properties of GO, the activation efficiency of nZVI on SPS was effectively improved when GO-NZVI was used as the activator. Compared with previous studies, the amounts of SPS and nZVI required for TCP degradation were significantly reduced.

(2) Optimizing injection methods in engineer-

ing practice. Compared with traditional injection wells, pressurized direct-push injection can effectively expand the influence radius of SPS and nZVI in soil and groundwater, thereby improving agent mass transfer and reducing required dosages.

(3) Combining with other remediation technologies. Compared with stand-along SPS advanced oxidation, combined technologies often achieve higher remediation efficiency. Some researchers have proposed combining bioremediation with SPS to address residual low-concentration pollutants in the environment. This not only enhances the remediation effect but also significantly reduces the amount of SPS required and lowers environmental risks.

(4) Other measures, such as adding SPS sustained-release agents or adjusting environmental conditions, can also help improve efficience.

In conclusion, when applying this technology to practical remediation projects, aquifer conditions should be comprehensively considered to determine the appropriate agent concentration, injection volumes, and injection methods (e.g. one-time injection or fractional injection), as well as other factors influencing the reaction.

3 Conclusion

Graphene oxide-modified nanoscale zero-valent iron composites were successfully prepared using the Hummer and polyphenol reduction method. The resulting material exhibited a porous and fluffy structure, with spherical nano-iron particles loaded on the surface of graphene oxide. The main component of the composites is α-Fe^0, with trace amounts of ferrous oxide, hydroxyl iron oxide and ferric tetroxide.

Modification with graphene oxide significantly enhanced the removal efficiency of nano-iron activated persulfate for TCP degradation. Within 1 hour, the TCP removal rate reached 67.2%, which is 78.2% higher than that of the unmodified system. The removal rate increased with higher persulfate concentrations. An appropriate C/Fe ratio in the graphene oxide modified nano-iron materials was found to improve persulfate activation, with the highest degradation efficiency observed at 10% C addition.

Using a graphene oxide-activated persulfate in-situ reaction zone to simulate the remediation of TCP contaminated groundwater, the TCP removal rate under different reaction conditions ranged from 30.1% to 73.3%. A larger particle size of the aquifer medium and a higher concentration of reactants were found to promote pollutant degradation, while a higher groundwater flow rate was not conducive to pollutant removal. The actual molar ratio of persulfate reacting with TCP ranged from 5.74:1 to 38.9:1, indicating that oxidant consumption is relatively high.

At actual contaminated sites, it is important to consider not only the remediation effectiveness but also the potential impact of chemical agents on the physicochemical properties of groundwater and the permeability of aquifers. To achieve green remediation and reduce secondary pollution, the reactivity of chemical agents should be further optimized. Moreover, additional exploration and research are needed on engineering measures for in-situ reaction zones, as well as on combined remediation technologies such as surfactant flushing or bioremediation techniques.

Acknowledgements

This study was financially supported by the Basal Research Fund of Chinese Academy of Geological Sciences (NO. SK202318), the Natural Science Foundation of Xiamen, China (No. 3502Z20 227309), and the Natural Science Foundation of Fujian Province of China (NO. 2023J01227).

References

Arslan-Alaton I, Koba-Ucun O. 2023. Treatment of reactive dye hydrolysates with UV-C- and ozone-activated percarbonate and persulfate. International Journal of Environmental Research, 17(6): 58−73. DOI: 10.1007/s41742-023-00548-4.

Boyandin AN, Bessonnva VA, Sukhanova AA, et al. 2024. Mechanism of thermochemical degradation of bacterial poly-3-hydroxybutyrate in solutions. Russian Chemical Bulletin, 73(3): 688−694. DOI: 10.1007/s11172-024-4179-9.

Braki ZA, Sohrabi MR, Motiee F. 2024. Application of central composite design for the simultaneous removal of tetracycline and cefixime using nanoscale zero-valent iron modified by montmorillonite and graphene oxide. Chemical Papers, 78(15): 8181−8193. DOI: 10.1007/s11696-024-03659-0.

Chen YT, Qie HT, Zhang YJ, et al. 2020. Synthesis of reduced graphene oxide supported zero-valent iron and its treatment of TNT waste-

water. Chemical Journal of Chinese University, 41(8): 1836−1842. DOI：10.7503/cjcu20200198.

Dai XL, Wang S, Li JB, et al. 2023. Reaearch progress on remediation technology of 1, 2, 3-trichloropropane contaminated groundwater. Applied Chemical Industry, 52(4): 1213−1224. DOI：10.16581/j.cnki.issn1671-3206.2023.04.026.

Deng Q, Li H, Han ZT, et al. 2019. Study on the removal efficiency of nano-sized iron particles produced by green tea reduction on Cr(VI) in simulated groundwater. South-North Water Transfers and Water Science & Technology, (1): 130−137. DOI：10.13476/j.cnki.nsbdqk.2019.0018.

Dombek T, Davis D, Stine J, et a1. 2004. Degradation of terbutylazine (2-chloro-4-ethylamino-6-terbutylamino-1, 3, 5-triazine) deisopropyl atrazine (2-amino-4-chloro-6-ethylamino-1, 3, 5-triazine) and chlorinated dimethoxy triazine (2-chloro-4, 6-dimethoxy-1, 3, 5-triazine) by zero valent iron and electrochemical reduction. Environmental Pollution, 129(6): 267−275. DOI：10.1016/j.envpol.2003.10.008.

Horlu M, Macit CK, Aksakal B, et al. 2024. Investigation of the effect of graphene oxide nanoparticles on the structural and dielectric parameters in zinc oxide semiconductors. Journal of Sol-Gel Science and Technology, 110(1): 169−182. DOI：10.1007/s10971-024-06350-8.

Huang XZ, Zhang YX, Zhang DS, et al. 2023. Reduced graphene oxide supported Fe/Ni nanocomposites for 2, 4-dichlorophenol removal. China Environmental Science, 43(12): 6352−6362. DOI：10.19674/j.cnki.issn1000-6923.2023.0207.

Jiang Y, Lu R, Chen Y, et al. 2024. Effect of Fe^{2+}-activated persulfate combined with biodegradation in removing gasoline BTX from karst groundwater: A box-column experimental study. Environmental Science and Pollution Research, 31(28): 50733−50745. DOI：10.1007/s11356-024-34597-9.

Li H, Han ZT, Deng Q, et al. 2023. Assessing the effectiveness of nanoscale zero-valent iron particles produced by green tea for Cr(VI)-contaminated groundwater remediation. Journal of Groundwater Science and Engineering, 11(1): 55−67. DOI：10.26599/JGSE.2023.9280006.

Li H, Han ZT, Ma CX, et al. 2015. Comparison of 1, 2, 3-trichloropropane reduction and oxidation by nanoscale zerovalent iron, zinc and activated persulfate. Journal of Groundwater Science and Engineering, 3(2): 156−163. DOI：10.26599/ JGSE.2015.9280018.

Li H, Qian Y, Han ZT, et al. 2023. Natural attenuation monitoring of 1, 2, 3- trichloropropane and benzene in the groundwater of organic pollution sites, Tianjin chemical plant and its environmental restoration suggestions. Geology in China, 50(5): 1446−1459. DOI：10.12029/gc20220302001.

Li H, Zhao YS, Han ZT, et al. 2015. Study on influence factors of remediation area of in-situ reaction zone injected with modified nano-iron. China Environmental Science, 35(4): 1135−1141.

Liu XM. 2018. Enhance degradation of polycyclic aromatic hydrocarbons with persulfate activation by nano zerovalent iron. Dalian: Dalin University of Technology.

Liu XY, Liu WT, Chi ZF. 2022. Reduced graphene oxide supported nanoscale zero-valent iron (nZVI/rGO) for in-situ remediation of Cr(VI)/nitrate-polluted aquifer. Journal of Water Process Engineering, 49: 103188−103203. DOI：10.1016/j.jwpe.2022.103188.

Merrill J P, Suchomel EJ, Varadhan S, et al. 2019. Development and validation of technologies for remediation of 1, 2, 3-trichloropropane in groundwater. Current Pollution Reports, 5(4): 1−10. DOI：10.1007/s40726-019-00122-7.

Ning Z, Zhang M, Zhang NN, et al. 2022. Metagenomic characterization of a novel enrichment culture responsible for dehalogenation of 1, 2, 3-trichloropropane to allyl chloride. Journal of Environmental Chemical Engineering, 10(6): 108907−108916. DOI：10.1016/j.jece.2022.108907.

Plessl K, Russ A, Vollprecht D. 2023. Application and development of zero-valent iron (ZVI) for groundwater and wastewater treatment. International Journal of Environmental Science and Technology, 20: 6913−6928. DOI：10.1007/s13762-022-04536-7.

Ren JG, Gao PC, Xu XJ, et al. 2021. Advances in

remediation technology for chlorinated hydrocarbons contamination in groundwater. Research of Environmental Science, 34(7): 1641−1653. DOI：10.13198/j.issn.1001-6929.2021.01.07.

Ren LM. 2019. Study on removal of chromium (VI) polluted groundwater using xanthan gum stabilized graphene oxide-supported nanoscale zero-valent iron. Changchun: Jilin University.

Sarathy V, Salter AJ, Nurmi JT, et al. 2010. Degradation of 1, 2, 3-trichloropropane (TCP): Hydrolysis, elimination, and reduction by iron and znic. Environmental Science and Technology, 44: 787−793. DOI：10.1021/es902595j.

Shang WX, Xu HY, Wang JW, et al. 2022. Microbial degradation of organochlorine pesticides. Chemistry and Bioengineering, 39(3): 12−18. DOI：10.3969/j.issn.1672-5425.2022.03.003.

Sun F, Zhu Y, Liu X, et al. 2023. Highly efficient removal of Se(IV) using reduced graphene oxide-supported nanoscale zero-valent iron (nZVI/rGO): Selenium removal mechanism. Environmental Science and Pollution Research, 30: 27560−27569. DOI：10.1007/s11356-022-24226-8.

Wang J, Liu X, Wang X, et al. 2022. Fe^{2+} activating persulfate selectively oxidized alcohols by biphasic/homogeneous reaction switch strategy. Chemical Papers, 76(11): 7229−7234. DOI：10.1007/s11696-022-02366-y.

Xing R. 2020. Performances and mechamisms of GO/nZVI nanocomposites for organic pollutants removal. Hangzhou: Zhejiang University. DOI：10.27461/d.cnki.gzjdx.2020.001991.

Xue W, Chen X, Liu H, et al. 2024. Activation of persulfate by biochar-supported sulfidized nanoscale zero-valent iron for degradation of ciprofloxacin in aqueous solution: Process optimization and degradation pathway. Environmental Science and Pollution Research, 31(7): 10950−10966. DOI：10.1007/s11356-024-31931-z.

Xue W, Li J, Chen X. et al. 2023. Recent advances in sulfidized nanoscale zero-valent iron materials for environmental remediation and challenges. Environmental Science and Pollution Research, 30(46): 101933−101962. DOI：10.1007/s11356-023-29564-9.

Yan SY, Chen YY, Xu HZ, et al. 2008. A novel advanced oxidation technology based on activated persulfate. Progress in Chemistry, 20(9): 1433−1437.

Yang XY, Yao C, Liu H, et al. 2018. Study on methylene blue removal by graphene oxide supported magnetic-nano iron. Technology of Water Treatment, 44(10): 53−57. DOI：10.16796/j.cnki.1000-3770.2018.10.011.

Yu C, Lu X, Lu J, et al. 2023. Degradation of amaranth by persulfate activated with zero-valent iron: Influencing factors, response surface modeling. SN Applied Sciences, 5(1): 1−14. DOI：10.1007/s42452-022-05097-7.

Zhang M. 2019. Degradation of 1, 2, 3-trichloropropane by activated sodium persulfate using nano iron suspension synthesized by green tea. Shijiazhuang: Hebei GEO university. DOI:10.27752/d.cnki.gsjzj.2019.000010.

Zhang M, Ning Z, Guo CJ, et al. 2023. Using compound specific isotope analysis to decipher the 1, 2, 3-trichloropropane-to-Allyl chloride transformation by groundwater microbial communities. Environmental Pollution, 316(1): 120577−120583. DOI：10.1016/j.envpol.2022.120577.